




Effect of Environmental Conditions on Quality Factors of MEMS Cantilever Beam Resonator in Gas Rarefaction

Minh Truong Phan¹ · Xuan Thang Trinh² · Quoc Cuong Le³ · Vo Ke Thanh Ngo² · Chi Cuong Nguyen^{1,2} 

Received: 2 November 2020 / Revised: 7 December 2020 / Accepted: 29 December 2020

© The Author(s), under exclusive licence to Springer Science+Business Media, LLC part of Springer Nature 2021

Abstract

This paper discussed the effect of environmental conditions (moisture and temperature) on the quality factors (Q -factor) of micro-electro-mechanical systems (MEMS) cantilever beam resonators in wide range of gas rarefaction (pressure (p), and accommodation coefficients (ACs)), and flexural mode of resonator. The modified molecular gas lubrication (MMGL) equation is applied for modeling the dominant squeeze film damping (SFD) problem on the quality factor of MEMS cantilever beam resonators to discuss the effect of environmental conditions. The external SFD and the internal structure damping (thermoelastic damping) and support loss) are accurately taken into account. Effective viscosity, which is ratio of dynamic viscosity and Poiseuille flow rate of moist air, is utilized to modify the MMGL equation to consider the environmental effects of moisture and temperature in gas rarefaction. In low pressures, mean free path changes more significantly with relative humidity and temperature than that of dynamic viscosity of moisture in gas rarefaction. Thus, effect of environmental conditions such as moisture and temperature must be discussed to improve Q -factors of MEMS cantilever beam resonators in wide range of gas rarefaction (p and ACs) and flexural modes of resonator. The results showed that Q -factor of SFD decreases significantly as moisture and temperature increase at higher gas rarefaction (lower p , and ACs), while Q -factor of SFD decreases and then increases slightly as moisture and temperature increase at lower gas rarefaction (higher p , and ACs). The total Q -factor is highly sensitive to the relative humidity and temperature in higher gas rarefaction (lower p and ACs) and lower flexural modes of resonator.

Keywords Quality factor · MEMS cantilever beam resonators · Temperature · Relative humidity · Gas rarefaction · Flexural mode of resonator

✉ Chi Cuong Nguyen
cuong.nguyenchi@shtplabs.org

Extended author information available on the last page of the article

1 Introduction

Cantilever beam is the most important structure of Micro-electro-mechanical systems (MEMS) resonator used in numerous miniaturized sensor and detector applications such as atomic force microscopy (AFM) tips [1], scanning force microscopy (SFM) [2], physical sensors (e.g. pressure, temperature, velocity, flow, frequency change) [3–6], chemical sensors (e.g. water vapor, protein adsorption) [7–9], bio-sensors (e.g. virus particles, bacterial, etc.) [10]. The other advantages are that MEMS cantilever beam resonators can operate in various environments such as liquids, gases, and vacuum. Therefore, these applications required a great enhancement in dynamic performance of MEMS cantilever beam resonators, which are fabricated in wide range of geometric parameters of micro/nano systems and excited at the fundamental mode up to high mode of resonators. However, the effects of environmental conditions (e.g. temperature, moisture, etc.) are main problems because dynamical performance of MEMS cantilever beam is strongly influenced by the viscous damping in air ambient environment.

In MEMS resonators, the most important dynamic characteristics are resonant frequency, damping factor, and quality factor (Q -factor). Physically, the Q -factor is defined as ratio of the stored energy of oscillators or resonators to rate of energy loss in a cycle of oscillation. Higher Q -factor (lower damping) is one of crucial requirement of MEMS resonators operated in high frequency stability and high sensitivity of sensing systems. The Q -factor of micro-cantilever resonator in liquids for chemical sensors and biosensors, which is very low to Q -factor ~ 1 in pure water and enhances in aqueous solution [11–14], is not exceeded 35 for transverse vibration [15, 16] because the density and viscosity of the fluids highly influenced on the cantilever's dynamic behavior and then high fluid damping produced. Due to the small Q -factor for the cantilevers in contact with the liquid samples, other designs of MEMS resonator array are used in these environments [17]. In this study, the Q -factor is enhanced by orders of magnitude using of cantilevers in gaseous environments. In MEMS cantilever beam resonators, there have been several damping mechanisms of oscillating structures that minimized the Q -factor of MEMS resonators. In air ambient environment, the external squeeze film damping (SFD), which is a dominant damping source appeared as the gas flow squeezed in small gas film spacing between two surfaces of vibrational structure and stationary substrate [18]. The internal structure damping sources such as the thermoelastic damping (TED) [19–22] and support loss [23, 24] are the other dominant damping mechanisms of MEMS cantilever beam resonators. These kinds of damping mechanisms (the SFD, TED and support loss) are dominant damping sources on the Q -factor of micro-cantilever beam resonators [25–27]. In literature review, the dynamic performances of MEMS resonators under the SFD problem have been studied with various physical parameters such as size [28], pressure [29], mode of resonator [30], gas medium [31], electrostatic driven force [32], etc. Therefore, the obtained results highlighted that to obtain high Q -factor of MEMS cantilever beam resonators in air ambient environment, the size of MEMS cantilever beam should be reduced and resonant frequency

must be operated as high as possible to minimize the energy loss due to the external SFD. To improve the Q -factor in air ambient condition, the gas rarefaction [33], surface roughness [34], and temperature [35] are considered as important effects on the Q -factors of MEMS resonators. Influence of relative humidity [36] on the quality factors of MEMS resonators is also discussed in wide range of gas rarefaction conditions. Besides, the effect of environmental conditions such as temperature and humidity of moist air has been found as strong effects on the dynamic performance of MEMS resonators in gas ambient conditions [37]. From a scientific point of view, the challenges in optimizing dynamic performance of MEMS resonators under gas ambient condition are to improve their sensitivity until the ultimate limit is reached. Therefore, the effect of environmental conditions (e.g. humidity, temperature, etc.) must be carefully considered as main effects of dynamic performance of MEMS cantilever beam resonators in a wide range of operating pressure conditions.

In gas atmospheric air condition, the density and viscosity of moist air, which are represented as functions of both moisture and temperature, can influence on the dynamic performance of MEMS resonators in air atmospheric pressure conditions [37]. Many studies have investigated the effect of temperature on the dynamic performance of MEMS resonators [26, 27, 38]. Few studies have considered the combined effects of temperature and humidity on the Q -factor of MEMS resonators in gas atmospheric air [39, 40]. The obtained results showed the Q -factor of MEMS resonators changed with temperature and humidity of moist air. However, the resultant Q -factor is very low in atmospheric pressure because high SFD produces in continuum gas flow conditions. To improve the Q -factor of resonators due to the SFD, the effect of gas rarefaction [33] is introduced. In gas rarefied flow, low pressure is introduced into very small gap film spacing (h) to reduce the SFD. The mean free path (λ) of gas flow changes considerably, then the slip flow takes place on the solid surfaces. To consider the gas rarefaction effect, the most useful method is the use of Poiseuille flow rate (Q_p) for gas rarefaction corrector. Some appropriate expressions of Q_p , which have been derived by solving the linearized Boltzmann equation (BGK model) for modeling the SFD to consider the gas rarefaction effects [33, 41–46]. Fundamentally, the effect of gas rarefaction characterized by the Knudsen number ($K_n = \lambda/h$) to represent for different gas rarefied flow regions (e.g., continuum, slip, transition, free molecular) as K_n varies from 0 to infinity. Also, effect of surface accommodation coefficients, ACs (α), which presents for the average tangential momentum exchanges of the gas molecular and solid surface interaction, is another important gas rarefaction parameter. Generally, the ACs vary from 0.1 to 1.0 depending on how incident molecules are scattered on solid surfaces by the diffuse or specular manners. In gas rarefied flow, the effect of ACs becomes significantly because Q_p changes considerably with the ACs in Nguyen and Li [33]. Also, in gas rarefied flow, the dynamic viscosity (μ) and mean free path (λ) of moist air changed significantly as functions of moisture and temperature. Therefore, the influences of moisture and temperature in gas rarefaction of air environment must be carefully considered to improve the Q -factor of resonators. Recently, Hasan [47] has addressed the effects of moisture and temperature on the dynamic response of MEMS resonators under the reduced pressure and the 1st mode shape. Moreover, the

effect of environmental conditions such as moisture and temperature on the Q -factors of MEMS cantilever beam resonators in wide range of gas rarefaction (inverse Knudsen number and accommodation coefficients) and high flexural modes of resonators is not considered. Also, the contributions of TED and support loss are not accurately included yet.

In the previous work, we solved the SFD problem of MEMS resonators using the modified molecular gas lubrication (MMGL) equation. Then, the quality factors of MEMS resonators are obtained by solving the MMGL equation and the transverse vibration equation of micro-structure with their corresponding boundary conditions simultaneously in the eigenvalue problem [33]. The expression of Poiseuille flow rate ($Q_p(D, \alpha_1, \alpha_2)$) is included to discuss the gas rarefaction effect in wide range of inverse Knudsen number, D ($0.01 \leq D \leq 100$) and accommodation coefficients, ACs ($0.1 \leq \alpha_1, \alpha_2 \leq 1.0$). Then, the effect of gas rarefaction and resonant mode are discussed on the Q -factor of MEMS resonators [33]. The effect of temperature [35] is discovered on the Q -factor of MEMS resonators in gas rarefaction. Also, influence of relative humidity on the Q -factor of MEMS resonator is also discussed in gas rarefaction [36]. However, the influence of environmental effects such as moisture and temperature of moist air on the Q -factor of MEMS resonators in gas rarefaction and flexural mode of resonator is not considered yet. In this paper, we investigate the change of quality factors of MEMS cantilever beam resonator as functions of temperature and humidity in wide range of gas rarefaction and flexural mode of resonator. Based on the previous works, the MMGL equation is modified with dynamic viscosity ($\mu(RH, T, p)$) of Morvay and Gvozdenac [48] and databases for Poiseuille flow rate ($Q_p(D(RH, T, p), ACs(\alpha_1, \alpha_2))$) of Li [44] for gas rarefaction corrector which changed as functions of temperature (T) and relative humidity (RH). Then, the combined effects of moisture and temperature of moist air are taken into account in gas rarefaction by including the dynamic viscosity ($\mu(RH, T, p)$) (Eqs.(13)-(15)) and the mean free path ($\lambda(RH, T, p)$) (Eq. 12) of moist air as functions of moisture and temperature. Also, the internal structural damping (TED and support loss) is accurately included. Finally, the influences of moisture and temperature are discussed on the Q -factors and Weighting of SFD of MEMS cantilever beam resonators in wide range of gas rarefaction (D , and ACs(α_1, α_2)) and flexural mode of resonator. The research objective is to develop a new approach to discuss the environmental effects such as temperature (T) and relative humidity (RH) on the quality factors of MEMS cantilever beam resonators in a wide range of flexural mode of resonator and gas rarefaction (pressure (p), and ACs (α_1, α_2)).

2 Governing Equation

2.1 The MMGL Equation for the SFD Problem

In gas environmental condition, harmonic vibration of micro-cantilever beam is restricted as a gas film trapped in small gap film spacing between a structure of micro-cantilever beam and a stationary substrate during their normal motion in the z direction.

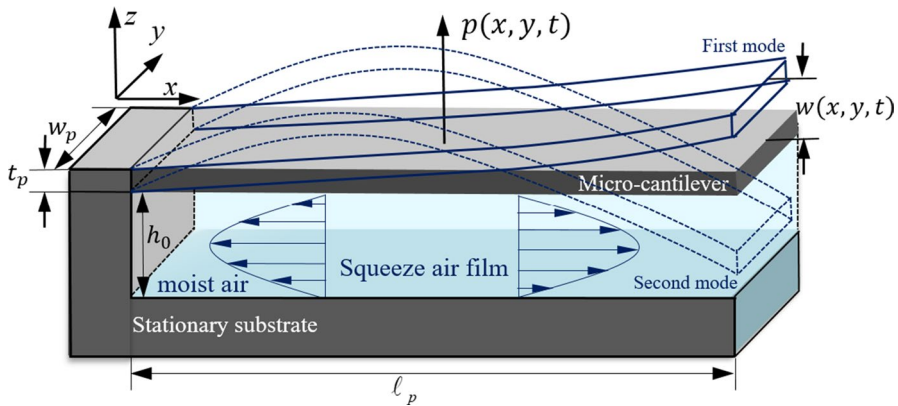


Fig. 1 A schematic of transverse motion of MEMS cantilever beam resonator with the first and second flexural mode shapes under the influence of SFD problem

Also, the Poiseuille flow rate (Q_p) of gas film between two parallel surfaces in small gas film spacing occurs as showed in Fig. 1.

Under a small gas film spacing, the pressure distribution of the SFD problem of the gas flow is obtained by solving a new modified molecular gas lubrication (MMGL) equation [33, 44] which is used to take into account the combined effects of moisture and temperature in wide range of gas rarefaction as follow

$$\frac{\partial}{\partial x} \left(\frac{\rho h^3}{12\mu_{eff}(RH, T, p)} \frac{\partial p}{\partial x} \right) + \frac{\partial}{\partial y} \left(\frac{\rho h^3}{12\mu_{eff}(RH, T, p)} \frac{\partial p}{\partial y} \right) = \frac{\partial}{\partial t} (\rho h) \quad (1)$$

where ρ is the gas density.

The effective viscosity (μ_{eff}) is used to modify the MMGL equation (Eq. (1)) considering the combined effects of moisture (RH) and temperature (T) in wide range of gas rarefaction as below

$$\mu_{eff}(RH, T, p) = \frac{\mu(RH, T, p)}{Q_p(RH, T, p)} \quad (2)$$

The complete database of Poiseuille flow rate ($Q_p(D, \alpha_1, \alpha_2)$) [44], which is numerically obtained by solving the linearized Boltzmann equation, is used to modify the MMGL equation to consider gas rarefaction effect in wide range of inverse Knudsen number, D ($0.01 \leq D \leq 100$) and accommodation coefficients, ACs ($0.1 \leq \alpha_1, \alpha_2 \leq 1.0$) conditions as follows:

$$\tilde{Q}_p(D, \alpha_1, \alpha_2) = \exp \left[\sum_{n=1}^{13} C_n (\ln D)^{13-n} \right] \quad (3)$$

$$Q_p = \frac{6}{D} \tilde{Q}_p \quad (4)$$

where $\tilde{Q}_p(D, \alpha_1, \alpha_2)$ is the Poiseuille flow rate for the gas rarefied flow. The present model is applicable to consider the combined effects of moisture (RH) and temperature (T) on MEMS devices and sensors in entire range of gas rarefaction (D , ACs (α_1, α_2)) conditions.

The inverse Knudsen number (D) is defined as ratio of the molecular mean free path length (λ) of gas to the gas film spacing (h) as follow

$$D = \frac{\sqrt{\pi}}{2K_n} = \frac{\sqrt{\pi}h}{2\lambda} \quad (5)$$

In moist air condition, the total pressure of moist air (p) [48, 49] is calculated as sum of partial pressure of dry air (p_a) and water vapor (p_w) as follow

$$p = p_a + p_w \quad (6)$$

The relative humidity (RH) [49, 50] of moist air is expressed as the ratio between the partial pressure of water vapor to the partial pressure of saturation water vapor (p_{sw}) at the actual dry bulk temperature as follow

$$RH = \frac{p_w}{p_{sw}} \cdot 100\% \quad (7)$$

The saturation pressure of water vapor (p_{sw}) is maximum pressure in which water vapor start to condensate at an actual temperature. Thus, p_{sw} [51, 52] is expressed as function of temperature as follow

$$p_{sw} = e^{(77.3450+0.0057 \cdot T-7235/T)/T^{8.2}} \quad (8)$$

Specific humidity [49] is also used to describe the properties of moist air in atmosphere as follow

$$x_s = 0.62198 \cdot p_w / (p - p_w) \quad (9)$$

where x_s is the specific humidity of moist air.

In the kinetic theory of gases [50], the mean free path of gas (λ) can be estimated as follow

$$\lambda = \frac{RT}{\sqrt{2\pi} \cdot N_a d^2 p} \quad (10)$$

where $R = 8.314$ (J/mol) is the gas constant, $N_a = 6.0221 \times 10^{23}$ is the Avogadro's number, M is the molecular weight of gas, and d is the diameter of the cross section of gas molecular at a stable state.

From Eq. (10), mean free path of gas (λ) [35] can be expressed as functions of pressure (p) and temperature (T) as following form

$$\frac{\lambda \cdot p}{T} = \frac{\lambda_0 \cdot p_0}{T_0} \quad (11)$$

where λ_0 is a reference mean free path of gas at a reference pressure of gas (p_0) and temperature (T_0).

At moist air, from Eqs.(6), (7), and (11), the mean free path of moist air (λ) can be expressed as follows

$$\lambda = \frac{\lambda_0 p_0 T}{p T_0} = \frac{\lambda_0 p_0 T}{(p_a + RH \cdot p_{sw}) T_0} \quad (12)$$

The dynamic viscosity of moist air (μ) at low pressure [48] is expressed as functions of pressure and temperature as follows

$$\mu = \frac{\mu_a}{1 + \Phi_{av} \cdot x_m} + \frac{\mu_v}{1 + \Phi_{va}/x_m} \quad (13)$$

where.

$$\Phi_{av} = \frac{[1 + (\mu_a/\mu_v)^{0.5} \cdot (m_v/m_a)^{0.25}]^2}{2\sqrt{2} \cdot (1 + m_a/m_v)^{0.5}}, \Phi_{va} = \frac{[1 + (\mu_v/\mu_a)^{0.5} \cdot (m_a/m_v)^{0.25}]^2}{2\sqrt{2} \cdot (1 + m_v/m_a)^{0.5}},$$

$x_m = 1.61 \times x_s$, m_a (=29) is molecular mass of dry air (kg/kmol), m_v (=18) is molecular mass of water vapor (kg/kmol).

The dynamic viscosity of dry air (μ_a) [48] under low pressure is

$$\mu_a = (a_1 + a_2 \cdot T - a_3 \cdot T^2 + a_4 \cdot T^3 - a_5 \cdot T^4) \times 10^{-6} \quad (14)$$

where $a_1 = 0.40401$, $a_2 = 0.074582$, $a_3 = 5.7171 \times 10^{-5}$, $a_4 = 2.9928 \times 10^{-8}$, $a_5 = 6.2524 \times 10^{-12}$.

The dynamic viscosity of water vapor (μ_v) [48] under low pressure is

$$\mu_v = (T/c_3)^{0.5} / (c_1 + c_2 \cdot (c_3/T) + c_4 \cdot (c_3/T)^2 - c_5 \cdot (c_3/T)^3) \times 10^{-6} \quad (15)$$

where $c_1 = 0.0181583$, $c_2 = 0.0177624$, $c_3 = 647.27$, $c_4 = 0.0105287$, $c_5 = 0.0036744$.

Therefore, the present model is a new approach to model the SFD problem considering the combined effects of moisture and temperature on the dynamic performance of MEMS resonators in wide range of gas rarefaction (inverse Knudsen number (D) and ACs (α_1, α_2)) conditions.

2.2 The Linear Equation of Motion for Transverse Vibration of Micro-Cantilever

In this section, a transverse vibration of micro-cantilever is resisted by a pressure force ($p(x, y, t)$) of gas film per unit area of micro-cantilever vibrated in z direction. A structure of micro-cantilever was mounted on a substrate at one side and free at the other sides as showed in Fig. 1. Under small amplitude of micro-cantilever (w), we can obtain the following linear form of equation of motion that governs for transverse vibration of the micro-cantilever [53, 54] as follow

$$D_p \left(\frac{\partial^4 w}{\partial x^4} + 2 \frac{\partial^4 w}{\partial x^2 \partial y^2} + \frac{\partial^4 w}{\partial y^4} \right) + \rho_m t_p \frac{\partial^2 w}{\partial t^2} = -p(x, y, t) \quad (16)$$

where $D_p(=Et_p^3/12(1 - \nu^2))$ is the cantilever rigidity, E is the Young’s modulus, ν is the Poisson’s ratio, t_p is the cantilever thickness, $w(x, y, t)$ is the transverse vibration of micro-cantilever at positions along the cantilever (x, y) , and time t , ρ_m is the material density of the cantilever.

The boundary conditions of a micro-cantilever are set with a fixed edge at one side $(x = 0)$ as follows.

$$w(0, y, t) \tag{17}$$

$$\frac{\partial w(0, y, t)}{\partial x} = 0 \tag{18}$$

and free edges at other sides $(x = \ell_p$ and $y=0, y = w_p)$ as follows

$$\frac{\partial^2 w(\ell_p, y, t)}{\partial x^2} = \frac{\partial^3 w(\ell_p, y, t)}{\partial x^3} = 0 \tag{19}$$

$$\frac{\partial^2 w(x, 0, t)}{\partial y^2} = \frac{\partial^3 w(x, 0, t)}{\partial y^3} = 0 \tag{20}$$

$$\frac{\partial^2 w(x, w_p, t)}{\partial y^2} = \frac{\partial^3 w(x, w_p, t)}{\partial y^3} = 0 \tag{21}$$

2.3 Quality Factors of MEMS Cantilever Beam Resonators

The Q -factor of MEMS resonators is obtained by calculating the resultant eigenvalue $(\lambda = \delta + i\omega)$. The calculated procedures of the eigenvalue problem can be found in Sect. 2.5 of Nguyen and Li [33]. In the eigenvalue problems [33], the Q -factor of SFD (Q_{SFD}) can be evaluated as the ratio between the resonant frequency (ω_0) (imaginary part of $\lambda(\text{Im}(\lambda))$) and the damping factor (δ) (real part of $\lambda(\text{Re}(\lambda))$) as follows

$$Q_{SFD} = \frac{\omega_0}{2\delta} = \left| \frac{\text{Im}(\bar{\lambda})}{2\text{Re}(\bar{\lambda})} \right| \tag{22}$$

For MEMS resonators in gas ambient condition, the total Q -factor (Q_T) can be evaluated by the main contributions of Q -factor components of SFD (Q_{SFD}), TED (Q_{TED}), and support loss (Q_{sup}) [26, 35], while the other damping mechanisms (e.g., surface loss, acoustic wave length loss, and material loss, etc.) can be neglected in wide range of gas rarefaction and flexural modes of resonator conditions as follows

$$\frac{1}{Q_T} = \frac{1}{Q_{SFD}} + \frac{1}{Q_{TED}} + \frac{1}{Q_{sup}} = \frac{1}{Q_{SFD}} + \frac{1}{Q_{int}} \tag{23}$$

where Q_{SFD} is obtained from the complex eigenvalue $(\bar{\lambda})$ by solving the linearized equations of Eq. (1), Eq. (16) with their appropriate boundary conditions (Eqs.

(17)-(21) in the eigenvalue problems [33]. Q_{TED} is calculated by the models of Zener [19, 20] (Eq. 14 in [35]), Lifshitz and Roukes [21] (LR model) (Eq. 15 in [35]) in Fig. 10 (Appendix A), and the FEM in COMSOL Multiphysics 5.5 [55] (Sect. 2.3 in [35]). Q_{sup} is obtained by the theoretical model of Hao et al. [23] (Eq. 18 in [35]) in Table 2 (Appendix B). Q_{int} is so-called internal structural damping which is the combined of TED and support loss in MEMS cantilever beam resonators.

Weighting of SFD ($Wt_{SFD}(\%)$), which is calculated as ratio between the contributions of the external SFD and the overall damping (SFD, TED, and support loss) as follows

$$Wt_{SFD}(\%) = \frac{(Q_{SFD})^{-1}}{(Q_T)^{-1}} = \frac{(Q_{SFD})^{-1}}{(Q_{SFD})^{-1} + (Q_{int})^{-1}} \quad (24)$$

where $Wt_{SFD}(\%)$ is the weighting of SFD, Q_{SFD}^{-1} is the external SFD, Q_{TED}^{-1} is the internal TED, and Q_{sup}^{-1} is the internal support loss. $(Q_{int})^{-1} = (Q_{TED})^{-1} + (Q_{sup})^{-1}$ is the internal structural damping of MEMS cantilever beam resonators.

2.4 Combined Effects of Moisture and Temperature on the Q-Factors of MEMS Cantilever Beam Resonators

In this study, to consider the combined effects of temperature (T) and relative humidity (RH) in gas rarefaction, the dynamic viscosity (μ) (Eqs.(13)-(15)) and the Poiseuille flow rate (Q_p) (Eq. 3) of moist air are calculated as functions of temperature (T) and relative humidity (RH) in wide range of gas rarefaction ($p_a = 100$ Pa and 100,000 Pa) conditions, respectively. Thus, the MMGL equation (Eq. 1) for the SFD problem is modified by using the effective viscosity, $\mu_{eff}(RH, T, p)$ (Eq. 2) which is defined as ratio between the dynamic viscosity, $\mu(RH, T, p)$ (Eqs.(13)-(15)) and the complete database of $Q_p(D(RH, T, p), \alpha_1, \alpha_2)$ (Eq. 3) in Li [44] to discuss the combined effects of temperature (T) and relative humidity (RH) in wide range of gas rarefaction (p , ACs(α_1, α_2)) on the Q -factors of MEMS cantilever beam resonators. Also, the Q -factors of internal structure damping problems (TED and support loss) are accurately taken into account to calculate the total Q -factor and weighting of SFD of MEMS cantilever beam resonators in wide range of temperature and flexural mode of resonator. In gas ambient condition, the Q -factors of MEMS cantilever beam resonators are significantly controlled by the external SFD in lower flexural modes of resonator. Whereas, the internal structural damping (e.g. TED and support loss) are the other dominant damping sources on the Q -factor of MEMS resonators in higher flexural modes of resonators [35]. Thus, the innovation of this study is investigation of the combined effects of temperature (T) and relative humidity (RH) on the Q -factor (Q_{SFD}), total Q -factor (Q_T), and Weighting of SFD ($Wt_{SFD}(\%)$) of MEMS cantilever beam resonator in wide range of gas rarefaction (p , ACs(α_1, α_2)) and flexural mode of resonator.

3 Results and Discussion

In this study, the influences of environmental effects such as moisture and temperature are simultaneously considered on the Q -factors of MEMS cantilever beam resonators in gas rarefaction. The basic geometric and operating conditions of MEMS cantilever beam resonator, which are used in this study, showed in Table 1.

3.1 Influence of Temperature and Relative Humidity on Effective Viscosity, μ_{eff} (RH,T,p)

In Fig. 2, the saturation water vapor pressure (p_{sw}) is plotted in wide range of ambient temperature ($200 \text{ K} < T < 380 \text{ K}$). The results showed that p_{sw} increases as T increases in wide range of temperature conditions. The obtained result can be used to calculate variations of relative humidity of moist air (Eq. 7) in wide range of ambient pressure (p_a) and temperature (T).

In Fig. 3, the dynamic viscosity of moist air (μ) in Eqs.(13)-(15) is plotted as functions of temperature (T) and relative humidity (RH) in wide range of gas rarefaction conditions. In Fig. 3a, μ is plotted as functions of temperature (T) and relative humidity (RH) at higher gas rarefaction ($p_a = 100 \text{ Pa}$). The results showed that μ of dry air increases with T because the dynamic viscosity of dry air (μ_a) in Eq. (14) increases with T . While, μ of moist air increases slightly with T because μ_a increases with T (μ_a is dominant at lower T region). Then, μ decreases significantly, and increases as T increases because μ_v in Eq. (15) increases with T (μ_v is dominant at higher T region). In Fig. 3b, the results showed that μ of dry

Table 1 Basic geometric and operating conditions of MEMS cantilever beam resonator used in this study

Symbol	Description	Values
ℓ_p	Length of cantilever beam	350 μm
w_p	Width of cantilever beam	22 μm
t_p	Thickness of cantilever beam	4 μm
E	Young's modulus of silicon cantilever beam [56]	$130 \times 10^9 \text{ Pa}$
ρ_m	Density of silicon cantilever beam [56]	2330 kg/m^3
ν	Poisson's ratio of silicon cantilever beam [56]	0.28
α_m	Thermal expansion coefficient of silicon cantilever beam	$2.6 \times 10^{-6} \text{ 1/K}$
κ	Thermal conductivity of silicon cantilever beam	90 W/(m.K)
C_p	Specific heat capacity of silicon cantilever beam	700 J/(kg.K)
h_0	Basic gas film thickness	4 μm
p_0	Reference ambient pressure of air	101,325 Pa
λ_{p_0}	Reference mean free path of air at pressure (p_0)	66.5 nm
T_0	Reference ambient temperature	300 K
T	Ambient temperature	200–380 K
RH	Relative humidity of moist air	0–100%
p_a	Ambient pressure of dry air	100–100,000 Pa

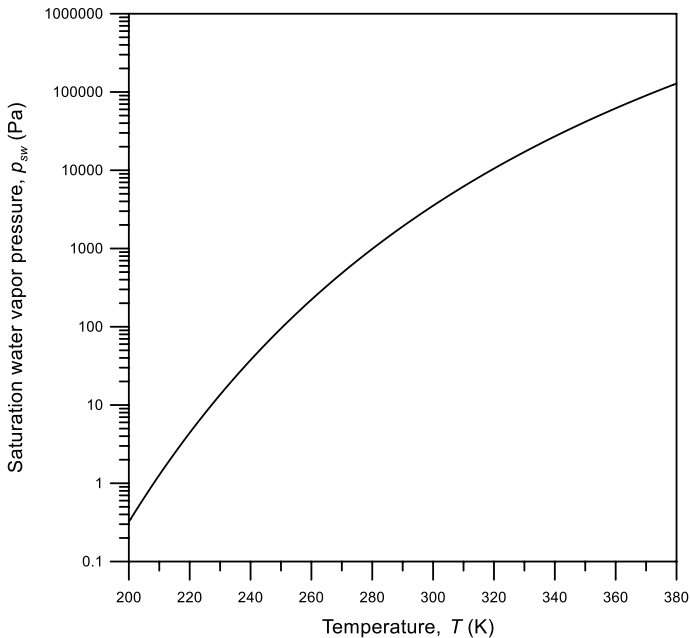


Fig. 2 Saturation water vapor pressure (p_{sw}) versus ambient temperature (T)

air increases with T , while μ of moist air increases up to a maximum value and then decreases slightly with T at low gas rarefaction ($p_a = 100,000$ Pa). Also, μ decreases as relative humidity (RH) increases in wide range of T and p_a conditions. Furthermore, the change of μ with T and RH is slightly at lower gas rarefaction ($p_a = 100,000$ Pa) while that change of μ with T and RH is significantly at higher gas rarefaction ($p_a = 100$ Pa). The obtained results of dynamic viscosity of moist air (μ) with different temperature (T) and relative humidity (RH) can be used to discuss the combined influences of moisture and temperature on quality factors of MEMS resonators in wide range of gas rarefaction conditions.

In Fig. 4, the Poiseuille flow rate (Q_p) of moist air (Eq. 3) is plotted as functions of temperature (T) for different relative humidity (RH) at different gas rarefaction (p_a) conditions. In Fig. 4a, the results showed that Q_p of dry air increases slightly with T , while Q_p of moist air decreases more significantly as T increases. Also, Q_p decreases as RH increases in wide range of T . In Fig. 4b, the results showed that Q_p of dry air increases with T , while Q_p of moist air increases up to a maximum value, then decreases slightly as T increases. Also, Q_p decreases as RH increases in wide range of T . Furthermore, the variation of Q_p with T and RH at higher gas rarefaction ($p_a = 100$ Pa) changes more significantly than that at lower gas rarefaction ($p_a = 100,000$ Pa). Thus, the influence of relative humidity (RH) on Q_p becomes more significantly at higher temperature (T) and higher gas rarefaction ($p_a = 100$ Pa) conditions. The obtained results of μ and Q_p with RH and T in gas rarefaction can be used to discuss the combined effects of moisture and

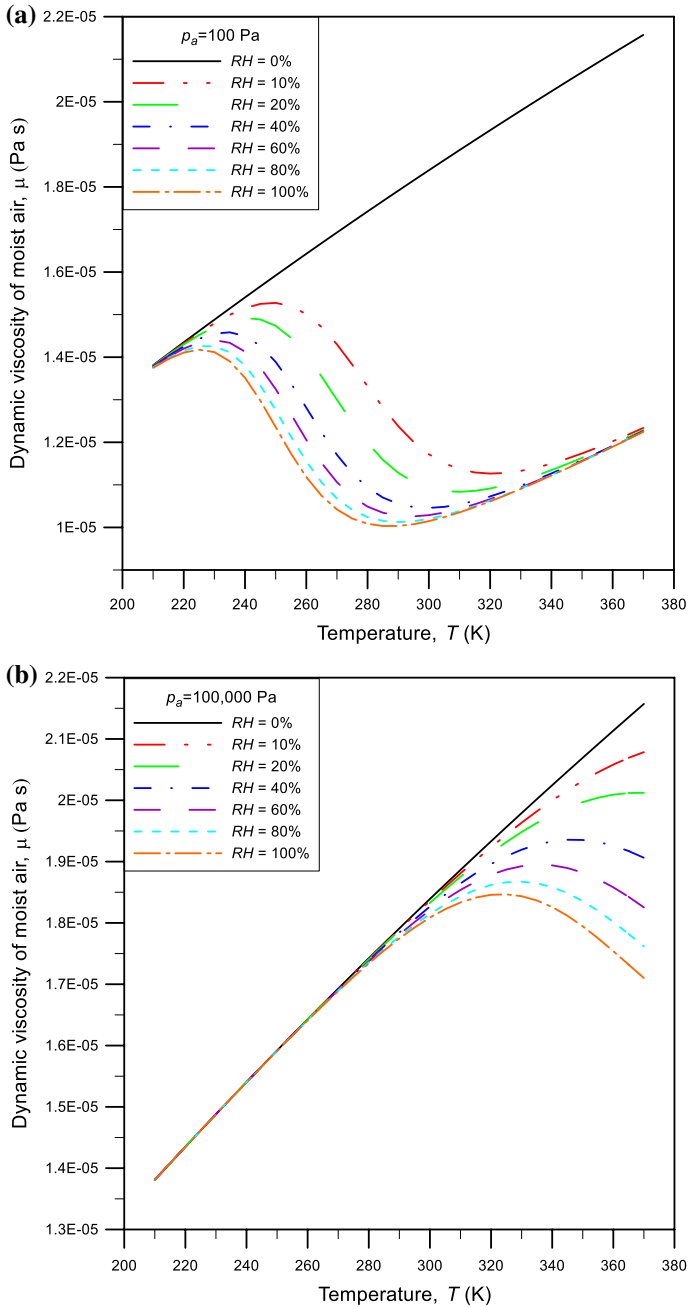


Fig. 3 Dynamic viscosity of moist air (μ) versus ambient temperature (T) for different relative humidity (RH) at a higher gas rarefaction ($p_a = 100$ Pa), **b** lower gas rarefaction ($p_a = 100,000$ Pa)

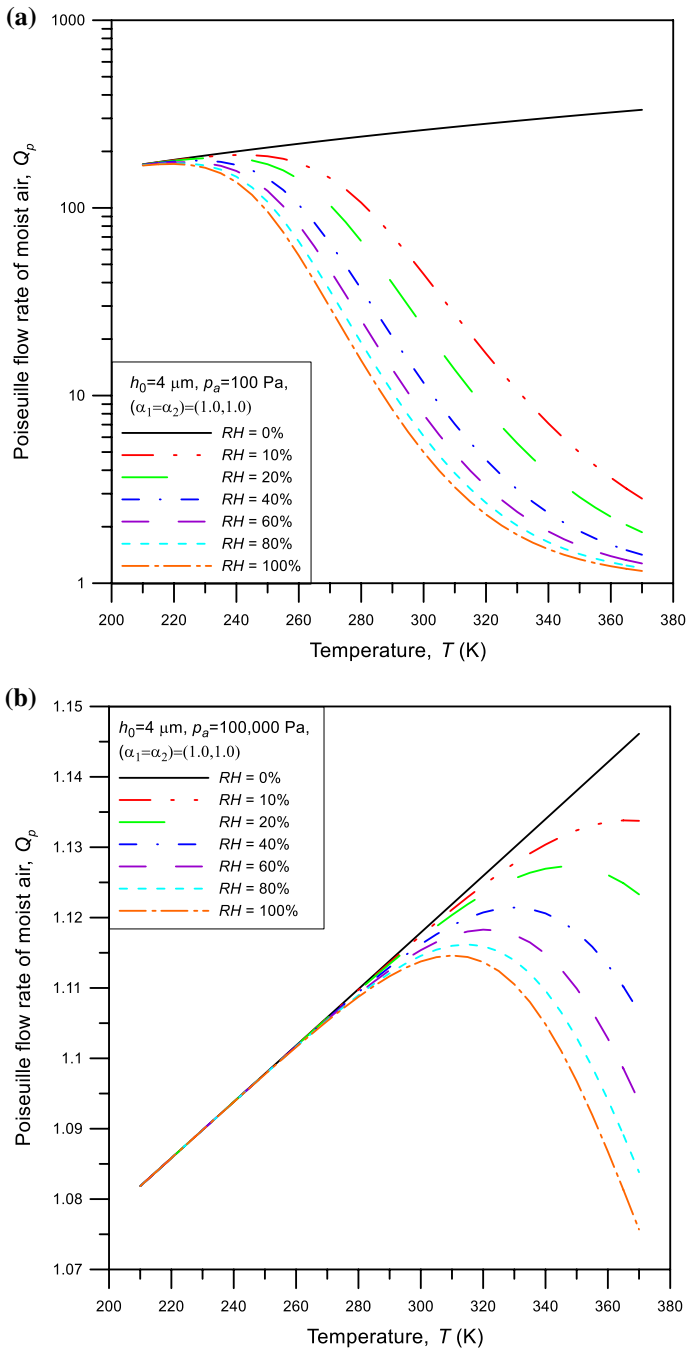


Fig. 4 Poiseuille flow rate (Q_p) of moist air versus ambient temperature (T) for different relative humidity (RH) at **a** higher gas rarefaction ($p_a = 100$ Pa), **b** lower gas rarefaction ($p_a = 100,000$ Pa)

temperature on the quality factors of MEMS cantilever beam resonators in wide range of gas rarefaction (p_a and ACs(α_1, α_2)) conditions.

In Fig. 5, the effective viscosity of moist air (μ_{eff}) in Eq. (2) is plotted as function of temperature (T) and relative humidity (RH) at different gas rarefaction (p_a) conditions. In Fig. 5a, the results showed that μ_{eff} of dry air decreases slightly with T , while μ_{eff} of moist air increases more significantly with T for different RH at higher gas rarefaction ($p_a = 100$ Pa). Also, μ_{eff} of moist air increases more considerably as RH increases in wide range of T conditions because Q_p of moist air decreases as RH and T increase. In Fig. 5b, μ_{eff} of dry air increases with T , while μ_{eff} of moist air increases up to a maximum value, then decreases slightly as T increases at lower gas rarefaction ($p_a = 100,000$ Pa) because μ of moist air increases up to a maximum value and then decreases slightly as T increases. Thus, the changes of the effective viscosity of moist air with the relative humidity (RH) and temperature (T) become more significantly in higher gas rarefaction, while its effect is very small in lower gas rarefaction. Thus, the variations of effective viscosity of moist air with temperature and relative humidity in wide range of gas rarefaction are very useful for a designer to optimize the Q-factors of MEMS cantilever resonators in wide range of gas rarefaction (p_a , ACs(α_1, α_2)) and flexural mode of resonator.

3.2 Influence of Temperature and Relative Humidity on Damping Factor (δ_{SFD}), and Quality Factor (Q_{SFD})

In Fig. 6, damping factor (δ_{SFD}) (real part of $\bar{\lambda}$) and the Q -factor of SFD ($Q_{SFD} = \omega_0/2\delta_{SFD}$) in Eq. (22) are plotted as functions of T and RH at different gas rarefaction ($p_a = 100$ Pa and 100,000 Pa) conditions. In Fig. 6a, the results showed that δ_{SFD} of dry air decreases slightly as T increases, whereas δ_{SFD} of moist air increases significantly as T and RH increase because Q_p of moist air decreases significantly as T and RH increase at higher gas rarefaction ($p_a = 100$ Pa). While, in Fig. 6b, δ_{SFD} increases and then decreases slightly as T and RH increase because μ of moist air increases and then decreases lightly as T and RH increase at lower gas rarefaction ($p_a = 100,000$ Pa). In Fig. 6c, at higher gas rarefaction ($p_a = 100$ Pa), the resultant Q -factor of SFD (Q_{SFD}) of dry air increases slightly with T , whereas Q_{SFD} of moist air decreases significantly as T and RH increase because δ_{SFD} of moist air increases significantly as T and RH increase at lower gas rarefaction ($p_a = 100$ Pa). Also, in Fig. 6d, Q_{SFD} of moist air decreases and then increases slightly as T and RH increase because δ_{SFD} increases and then decreases slightly as T and RH increase at lower gas rarefaction ($p_a = 100,000$ Pa). Thus, the obtained results can be useful to explain the influences of moisture and temperature on the quality factor of SFD (Q_{SFD}), total quality factor (Q_T), and Weighting of SFD ($Wt_{SFD}(\%)$) of MEMS cantilever beam resonator in wide range of gas rarefaction (p_a , ACs(α_1, α_2)) and flexural mode of resonator.

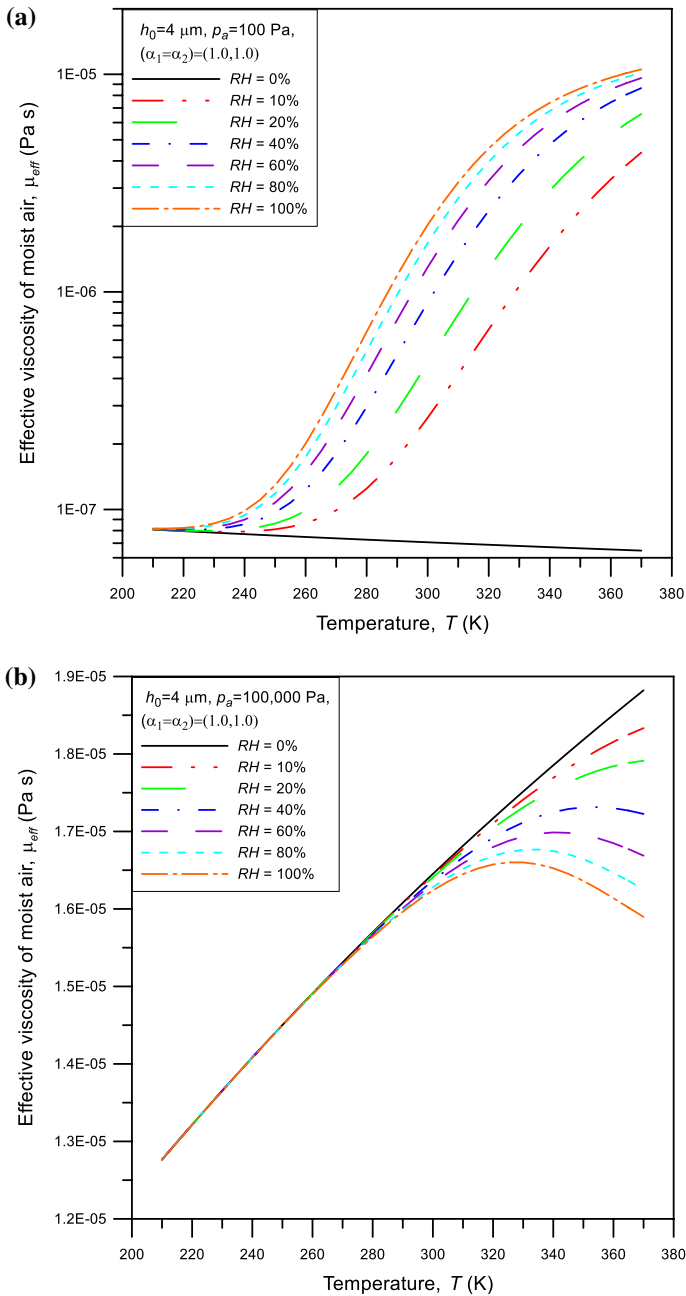


Fig. 5 Effective viscosity (μ_{eff}) of moist air versus ambient temperature (T) for different relative humidity (RH) at **a** higher gas rarefaction ($p_a = 100 \text{ Pa}$), **b** lower gas rarefaction ($p_a = 100,000 \text{ Pa}$)

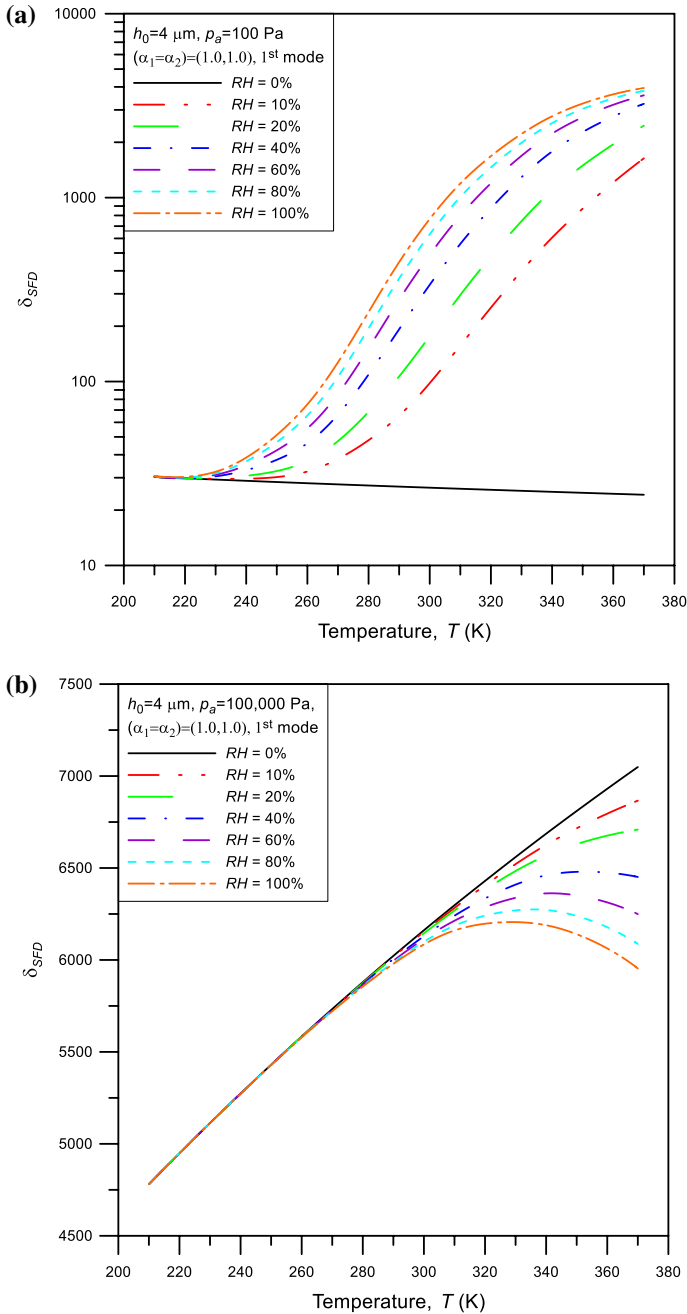


Fig. 6 **a** Damping factor of SFD (δ_{SFD}) at higher gas rarefaction ($p_a = 100 \text{ Pa}$), **b** damping factor of SFD (δ_{SFD}) at lower gas rarefaction ($p_a = 100,000 \text{ Pa}$), **c** Q -factor of SFD (Q_{SFD}) at higher gas rarefaction ($p_a = 100 \text{ Pa}$), **d** Q -factor of SFD (Q_{SFD}) at lower gas rarefaction ($p_a = 100,000 \text{ Pa}$) versus ambient temperature (T) for different relative humidity (RH)

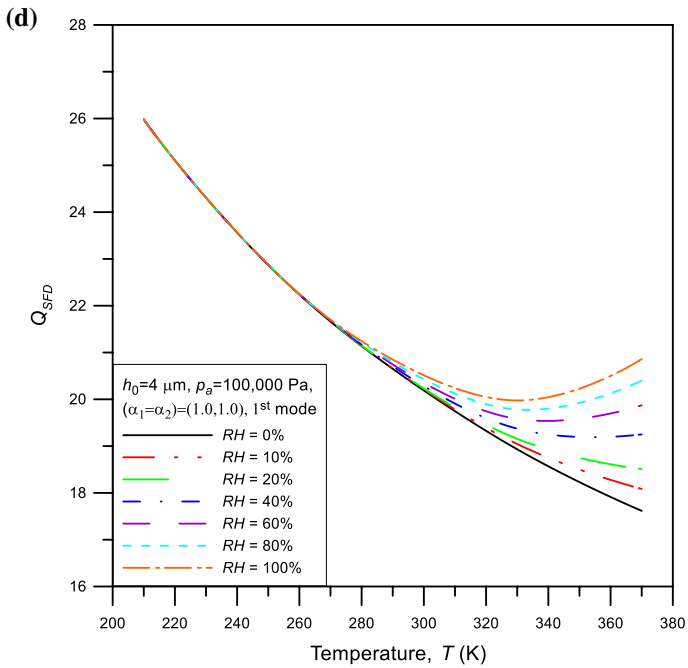
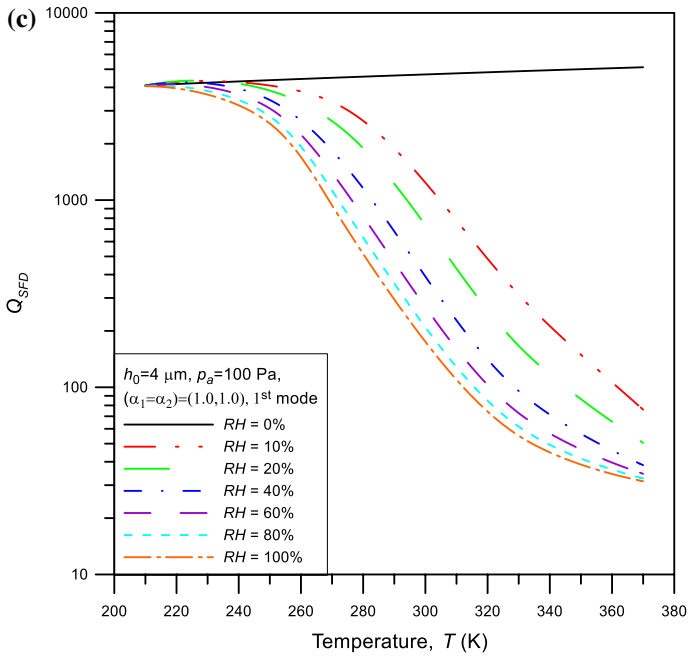


Fig. 6 (continued)

3.3 Influence of Temperature and Relative Humidity on Quality Factor Q_{SFD} , Q_T and $Wt_{SFD}(\%)$

In Fig. 7, ratio of Q -factor of moist air and dry air ($Q_{SFD_moist}/Q_{SFD_dry}$) is discussed as functions of temperature (T) and relative humidity (RH) in wide range of gas rarefaction (p_a , ACs($\alpha_1 = \alpha_2$)) conditions. In Fig. 7a, $Q_{SFD_moist}/Q_{SFD_dry}$ is plotted with T and RH in various gas rarefaction (p_a) conditions. The results showed that ratio of $Q_{SFD_moist}/Q_{SFD_dry}$ decreases significantly as T and RH increase because Q_{SFD_moist} decreases significantly as T and RH increase at higher gas rarefaction ($p_a = 100$ Pa, 1000 Pa, 10,000 Pa). Whereas, ratio of $Q_{SFD_moist}/Q_{SFD_dry}$ increases slightly as T and RH increase because Q_{SFD_moist} increases slightly as T and RH increase at lower gas rarefaction ($p_a = 100,000$ Pa). Also, influences of temperature (T) and relative humidity (RH) on ratio of $Q_{SFD_moist}/Q_{SFD_dry}$ become significantly at higher gas rarefaction (lower p_a) conditions. In Fig. 7b, $Q_{SFD_moist}/Q_{SFD_dry}$ is plotted with T in various gas rarefaction (p_a , and ACs ($\alpha_1 = \alpha_2$)) conditions. The results showed that $Q_{SFD_moist}/Q_{SFD_dry}$ decreases more considerably as T increases and ACs ($\alpha_1 = \alpha_2$) decrease at higher gas rarefaction ($p_a = 100$ Pa, 1000 Pa, 10,000 Pa). Whereas, $Q_{SFD_moist}/Q_{SFD_dry}$ increases slightly with T and ACs ($\alpha_1 = \alpha_2$) increase at lower gas rarefaction ($p_a = 100,000$ Pa). Thus, influence of moisture and temperature on ratio of $Q_{SFD_moist}/Q_{SFD_dry}$ becomes significantly at higher gas rarefaction (lower p_a and ACs($\alpha_1 = \alpha_2$)), while this influence reduces in lower gas rarefaction (higher p_a and ACs($\alpha_1 = \alpha_2$)) conditions.

In Fig. 8, ratio of $Q_{SFD_moist}/Q_{SFD_dry}$ and Q_{T_moist}/Q_{T_dry} is calculated as functions of temperature (T) for different flexural modes of resonator at higher gas rarefaction ($p_a = 100$ Pa). In Fig. 8a, the results showed that $Q_{SFD_moist}/Q_{SFD_dry}$ decreases as T increases for different flexural modes of resonator. Variations of $Q_{SFD_moist}/Q_{SFD_dry}$ with T are unchanged for different flexural modes of resonator. In Fig. 8b, the total Q -factor (Q_T) is calculated by Eq. (23) by the contributions of Q -factor of SFD, TED (Fig. 10 in Appendix A) and support loss (Table 2 in Appendix B), respectively. The ratio of total Q -factor of moist air and dry air (Q_{T_moist}/Q_{T_dry}) is plotted as functions of temperature (T) for different flexural modes of resonator at higher gas rarefaction ($p_a = 100$ Pa). The results showed that Q_{T_moist}/Q_{T_dry} decreases significantly with T for various flexural modes of resonator because Q_{SFD} of moist air (Fig. 6) and Q_{TED} (Fig. 10) decrease as T increases. Also, Q_{T_moist}/Q_{T_dry} decreases more significantly with T at lower flexural modes of resonator because SFD is dominant at lower flexural mode of resonator conditions (Q_{SFD} of moist air decreases with T more significantly than that of Q_{int} as the mode decreases). While Q_{T_moist}/Q_{T_dry} changes slightly with T at higher flexural mode of the resonator because the TED and support loss increase and become dominant at higher flexural mode of the resonator (Q_{TED} and Q_{anch} decrease as the mode increases). Thus, Q_{T_moist}/Q_{T_dry} decreases with T more significantly at lower modes of resonator, while this variation becomes slightly at higher modes of resonator. The quality factor of MEMS cantilever beam resonators becomes very sensitive to changes in moisture and temperature at higher gas rarefaction and lower flexural mode of resonator.

In Fig. 9, Weighting of SFD ($Wt_{SFD}(\%)$) in Eq. (24) is introduced to investigate the combined effects of relative humidity (RH) and temperature (T) on the dynamic

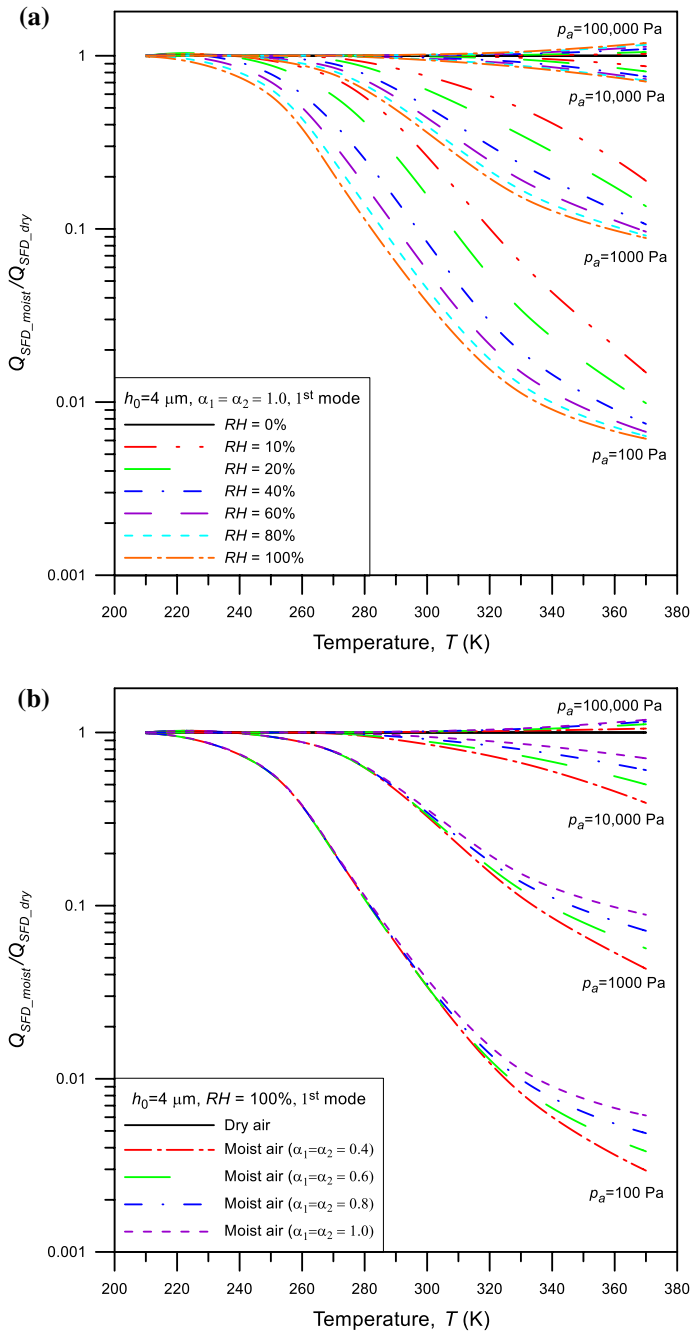


Fig. 7 Ratio of $Q_{SFD_moist}/Q_{SFD_dry}$ versus temperature (T) for different **a** Relative humidity (RH), **b** Accommodation coefficients, ACs ($\alpha_1 = \alpha_2$) under various gas rarefaction conditions

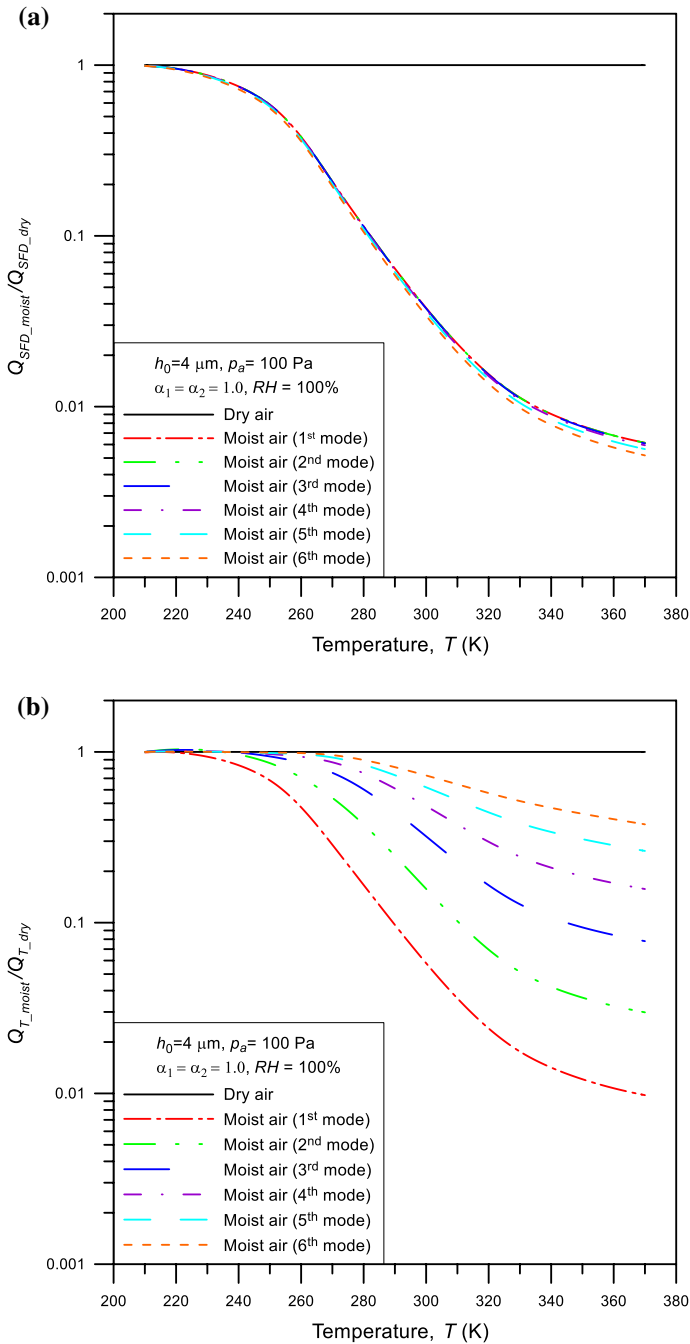


Fig. 8 **a** Ratio of $Q_{SFD_moist}/Q_{SFD_dry}$, **b** ratio of Q_{T_moist}/Q_{T_dry} versus temperature (T) for various flexural mode of resonator conditions

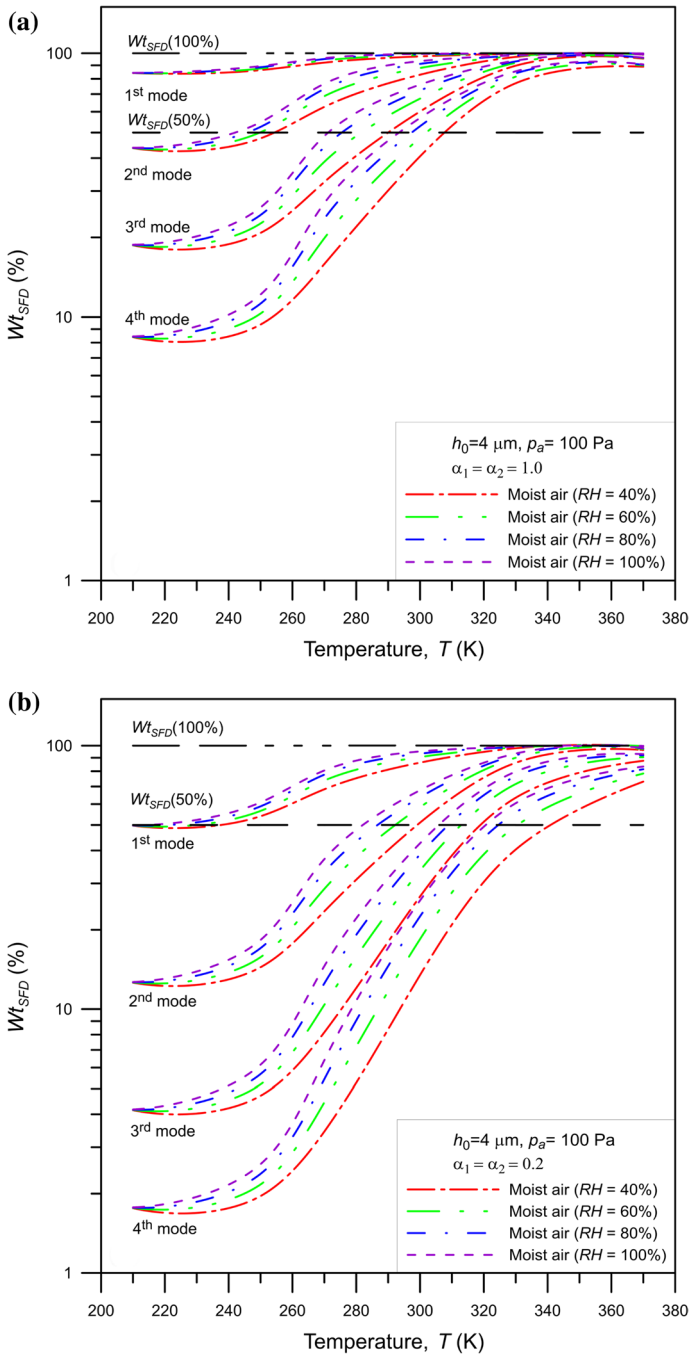


Fig. 9 Weighting of SFD ($Wt_{SF D}(\%)$) versus temperature (T) and relative humidity (RH) with different mode of resonator for different gas rarefaction of **a** ACs(1.0,1.0), **b** ACs(0.2,0.2)

performance of MEMS cantilever beam resonators in wide range of gas rarefaction ($ACs(\alpha_1, \alpha_2)$) and flexural mode of resonator. The results showed that $Wt_{SFD}(\%)$ increases as T and RH increase because SFD increases ($(Q_{SFD})^{-1}$ increases) as T and RH increase (the gas flow becomes more restricted as T and RH increase). Also, influences of T and RH on $Wt_{SFD}(\%)$ seem unchanged in the 1st mode of vibration in which the SFD is significantly and contribution of the SFD ($(Q_{SFD})^{-1}$) on total damping ($(Q_T)^{-1}$) is very dominant. Whereas, influences of T and RH on $Wt_{SFD}(\%)$ become more significantly as flexural mode of resonator increases because the contribution of SFD ($(Q_{SFD})^{-1}$) with T and RH reduces significantly, while the contribution of TED ($(Q_{TED})^{-1}$) and support loss ($(Q_{sup})^{-1}$) on total damping ($(Q_T)^{-1}$) becomes more dominantly at higher flexural mode of resonators and higher gas rarefaction ($p_a = 100$ Pa). Furthermore, the influence of T and RH on $Wt_{SFD}(\%)$ becomes more considerably in wide range of mode of resonator as the gas rarefaction increases from $ACs(1.0, 1.0)$ (Fig. 9a) to $ACs(0.2, 0.2)$ (Fig. 9b). Thus, the influence of moisture and temperature on $Wt_{SFD}(\%)$ is neglected at the 1st mode of resonator, while this influence becomes more significantly at higher flexural mode of resonator and higher gas rarefaction (lower p_a and $ACs(\alpha_1, \alpha_2)$). Finally, influence of temperature (T) and relative humidity (RH) on Q_T of moist air becomes more significantly in higher gas rarefaction (lower p_a , $ACs(\alpha_1, \alpha_2)$) and lower flexural mode of resonator.

4 Conclusions

In this study, the quality factor of SFD problem of MEMS cantilever beam resonators is obtained by solving the MMGL equation (Eq. 1), equation of motion of micro-cantilever (Eq. 16), and their appropriate boundary conditions (Eqs.(17)-(21)) in the eigen-value problem, simultaneously. The dynamic viscosity ($\mu(RH, T, p)$) (Eqs.(13)-(15)) and Poiseuille flow rate, $Q_p(D(RH, T, p), ACs(\alpha_1, \alpha_2))$ of moist air (Eq. (3)) are utilized to modify the MMGL equation to consider the combined effects of moisture and temperature in gas rarefaction. The quality factors of internal structure damping problems (TED and support loss) of MEMS cantilever beam resonators are also taken into account. Thus, influence of environmental effects such as moisture and temperature of moist air on the Q -factor (Q_{SFD} , Q_T), and $Wt_{SFD}(\%)$ of MEMS cantilever beam resonators is discussed in wide range environmental conditions of relative humidity ($0\% \leq RH \leq 100\%$), temperature ($200 \text{ K} \leq T \leq 380 \text{ K}$), pressure ($100 \text{ Pa} \leq p_a \leq 100,000 \text{ Pa}$), and $ACs(0.1 \leq \alpha_1, \alpha_2 \leq 1.0)$ conditions. Some remarkable outcomes are listed as below.

- The Q -factor increases considerably as temperature (T) and relative humidity (RH) decrease at higher gas rarefaction (lower p_a , $ACs(\alpha_1, \alpha_2)$) in the 1st mode of resonator.
- Influence of environmental effect such as moisture and temperature on the Q -factor becomes more significantly in higher gas rarefaction and lower flexural mode of resonator. While, this effect on the Q -factor reduces considerably in lower

gas rarefaction (higher p_a , $ACs(\alpha_1, \alpha_2)$) and higher flexural mode of resonator. These obtained results can be used to design high sensitivity of MEMS sensors for temperature, and moisture sensing applications based on the cantilever beam structure operating in wide range of gas rarefaction (p , $ACs(\alpha_1, \alpha_2)$) and flexural mode of resonator.

Acknowledgments This research was supported by the Institute for Computational Science and Technology (ICST), Contract Number: 08/2019/HĐ-KHCNTT in October 24th, 2019 and series number: 082019-311.

Appendix A

In Fig. 10, the Q factor of TED (Q_{TED}) is calculated as function of temperature (T) for various flexural modes of cantilever beam resonator. The result showed that Q_{TED} decreases as T increases for different modes of resonator. Also, Q_{TED} decreases more significantly as flexural modes of resonator increases because the TED increases with T and becomes dominantly in higher flexural mode of resonator. The calculated results of Q_{TED} from the present LR model [11] (Eq. 15 in [35]) showed good agreement with those obtained results from the Zener models [19, 20] (Eq. 14 in [35]), and those obtained results with COMSOL Multiphysics 5.5 [55] (Sect. "Quality Factors of MEMS Cantilever Beam Resonators" in [35]) in wide range of temperatures

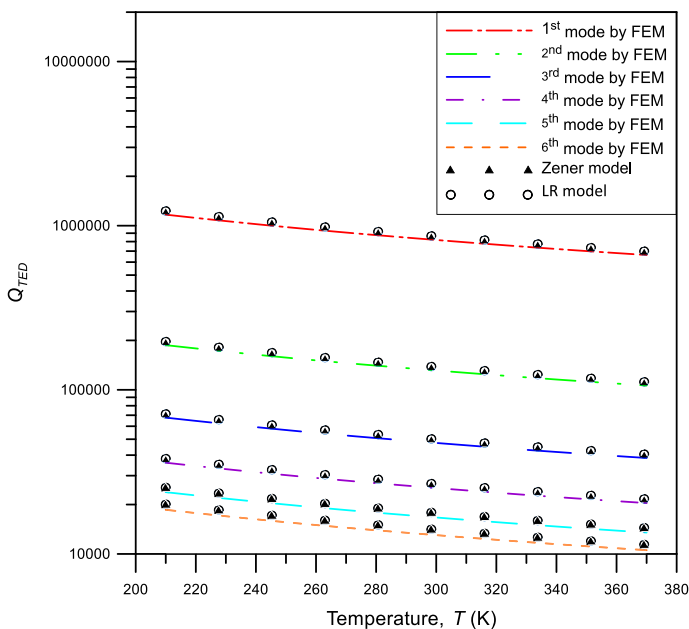










Fig. 10 The Q -factor of TED (Q_{TED}) versus temperature (T) for different flexural mode of resonator

and resonator modes. Thus, the obtained results of Q_{TED} from the LR model, which are used in the present analysis, can be applied to calculate the total Q factor (Q_T) of MEMS cantilever beam resonators in wide range of temperature and flexural mode of resonator.

Appendix B

In Table 2, Q_{sup} is calculated by the model of Hao et al. [23] (Eq. 18 in [35]) for various flexural mode of MEMS cantilever beam resonator. The validation of this model has been proved by the assumption that the width of cantilever beam (w_p) is much less than the transverse elastic wavelength (λ_T) ($\lambda_T/w_p \gg 1$). The result showed that Q_{sup} decreases significantly as the mode of resonator increases because the support loss becomes a dominant source of energy loss on MEMS resonators in higher flexural mode of resonator. Thus, the results of Q_{sup} can be used to calculate the total Q -factor (Q_T) of MEMS cantilever beam resonator in wide range of flexural mode of resonator conditions.

Table 2 The quality factor of support loss (Q_{sup}) for various flexural mode of MEMS cantilever beam resonator

Flex- ural mode	Mode Shape	Resonant freq. f_n [Hz]	λ_T	$C_{F(n)}$	$\frac{\lambda_T}{w_p} \gg 1$	Q_{sup}
1st		39,543	0.118	2.081	5366.28	1,394,107
2nd		247,675	0.0189	0.173	856.78	115,896
3rd		693,074	0.00674	0.064	306.18	42,875
4th		1,357,134	0.00344	0.033	156.36	22,107
5th		2,241,420	0.00208	0.020	94.67	13,398
6th		3,344,642	0.00139	0.013	63.45	8,708
7th		4,665,292	0.00100	0.009	45.49	6,029
8th		6,201,410	7.53e-4	0.007	34.22	4,689

References


1. Binnig, G., & Quate, C. F. (1986). Atomic force microscope. *Physical Review Letters*, 56(9), 930–934.
2. Thundat, T., Warmack, R. J., Chen, G. Y., & Allison, D. P. (1994). Thermal and ambient-induced deflections of scanning force microscope cantilevers. *Applied Physics Letters*, 64, 2894–2896.
3. Takahashi, H., Dung, N. M., Matsumoto, K., & Shimoyama, I. (2012). Differential pressure sensor using a piezoresistive cantilever. *Journal of Micromechanics and Microengineering*, 22, 055015–055021.
4. Chennippan, M., Bhaskaran, P. E., Adhulrasheed, I. S. K., Subramaniam, T., & Govindasamy, R. (2020). Vibration signals based bearing defects identification through online monitoring using LABVIEW. *Journal Européen des Systèmes Automatisés*, 53, 187–193.
5. Priyanka, E. B., Maheswari, C., Ponnibala, M., & Thangavel, S. (2019). SCADA based remote monitoring and control of pressure & flow in fluid transport system using IMCPID controller. *Advances in Systems Science and Applications*, 03, 140–162.
6. Priyanka, E. B., Thangavel, S., & Pratheep, V. G. (2020). Enhanced digital synthesized phase locked loop with high frequency compensation and clock generation. *Sensing and Imaging*, 21–43.
7. Baller, M. K., Lang, H. P., Fritz, J., Gerber, Ch., Gimzewski, J. K., Drechsler, , et al. (2000). A cantilever array-based artificial nose. *Ultramicroscopy*, 82, 1–9.
8. Lang, H. P., Hegner, M., & Gerber, C. (2005). Cantilever array sensors. *Materialstoday*, 8(4), 30–36.
9. Pratheep, V. G., Priyanka, E. B., & Prasad, P. H. (2019). Characterization and analysis of natural fibre-rice husk with wood plastic composites. *IOP Conf. Series: Materials Science and Engineering*, 561, 012066.
10. Gupta, A., Akin, D., & Bashir, R. (2004). Single virus particle mass detection using microresonators with nanoscale thickness. *Applied Physics Letters*, 84(11), 1976–1978.
11. Tamayo, J., Humphris, A. D. L., Malloy, A. M., & Miles, M. J. (2001). Chemical sensors and biosensors in liquid environment based on microcantilevers with amplified quality factor. *Ultramicroscopy*, 86, 167–173.
12. Cyril, V., Isabelle, D., Stephen, M. H., Fabien, J., & Andreas, H. (2008). Analysis of resonating microcantilevers operating in a viscous liquid environment. *Sensors and Actuators A*, 141, 43–51.
13. Singh, P., & Yadava, R. D. S. (2020). Stochastic resonance induced performance enhancement of MEMS cantilever biosensors. *J. Phys. D: Appl. Phys.* 53(46).
14. Fischeneder, M., Kucera, M., Hofbauer, F., Pfusterschmid, G., Schneider, M., & Schmid, U. (2018). Q-factor enhancement of piezoelectric MEMS resonators in liquids with active feedback. *Sensor Actuat B-Chem.*, 260, 198–203.
15. Blake, N. J., & Raj, M. (2012). Biosensing using dynamic-mode cantilever sensors: A review. *Bio-sensors & Bioelectronics*, 32(1), 1–18.
16. Schneider, M., Pfusterschmid, G., Patocka, F., & Schmid, U. (2020). High performance piezoelectric AlN MEMS resonators for precise sensing in liquids. *Elektrotechnik & Informationstechnik.*, 137(3), 121–127.
17. Amin, E., Habib, B. G., & Mousa, S. (2019). A Novel biosensor based on micromechanical resonator array for lab-on-a-chip applications. *Sensing and Imaging*, 20, 39.
18. Hosaka, H., Itao, K., & Kuroda, S. (1995). Damping characteristics of beam-shaped micro-oscillators. *Sensors and Actuators A: Physical*, 49(1–2), 87–95.
19. Zener, C. (1937). Internal friction in solids I theory of internal friction in reeds. *Physical Review*, 52(3), 230–235.
20. Zener, C. (1938). Internal friction in solids II general theory of thermoelastic internal friction. *Physical Review*, 53(1), 90–99.
21. Lifshitz, R., & Roukes, M. L. (2000). Thermoelastic damping in micro- and nanomechanical systems. *Physical Review B*, 61(8), 5600–5609.
22. Zhou, H., Li, P., & Zuo, W. (2016). Thermoelastic damping in microwedged cantilever resonator with rectangular cross-section. In: *IEEE 2016 int. conf. on mechatronics and automation (ICMA)*, Harbin, China, 1590–1595.
23. Hao, Z., Erbil, A., & Ayazi, F. (2003). An analytical model for support loss in micromachined beam resonators with in-plane flexural vibrations. *Sensors and Actuators A: Physical*, 109(1–2), 156–164.

24. Jandak, M., Neuzil, T., Schneider, M., & Schmid, U. (2016). Investigation on different damping mechanisms on the Q factor of MEMS resonators. *Procedia Engineering*, 168, 929–932.
25. Yang, J., Ono, T., & Esashi, M. (2002). Energy dissipation in submicrometer thick single-crystal silicon cantilevers. *Journal of Microelectromechanical Systems*, 11(6), 775–783.
26. Kim, B., Hopcroft, M. A., Candler, R. N., Jha, C. M., Agarwal, M., Melamud, R., et al. (2008). Temperature dependence of quality factor in MEMS resonators. *Journal of Microelectromechanical Systems*, 17(3), 755–766.
27. Ghaffari, S., Ng, E. J., Ahn, C. H., Yang, Y., Wang, S., Hong, V., et al. (2015). Accurate modeling of quality factor behavior of complex silicon MEMS resonators. *Journal of Microelectromechanical Systems*, 24(2), 276–288.
28. Lee, J. W. (2011). Analysis of fluid-structure interaction for predicting resonant frequencies and quality factors of a microcantilever on a squeeze-film. *Journal of Mechanical Science and Technology*, 25(5), 3005–3013.
29. Bao, M., & Yang, H. (2007). Squeeze film air damping in MEMS. *Sensors and Actuators A: Physical*, 136(1), 3–27.
30. Pandey, A. K., & Pratap, R. (2007). Effect of flexural modes on squeeze film damping in MEMS cantilever resonators. *Journal of Micromechanics and Microengineering*, 17(12), 2475–2484.
31. Kim, S. J., Dean, R., Jackson, R. L., & Flowers, G. T. (2011). An investigation of the damping effects of various gas environments on a vibratory MEMS device. *Tribology International*, 44(2), 125–133.
32. Burg, T. P., & Manalis, S. R. (2003). Suspended microchannel resonators for biomolecular detection. *Applied Physics Letters*, 83(2), 2698–2700.
33. Nguyen, C. C., & Li, W. L. (2016). Effect of gas rarefaction on the quality factors of micro-beam resonators. *Microsystem Technologies*, 23, 3185–3199.
34. Nguyen, C. C., & Li, W. L. (2016). Effects of surface roughness and gas rarefaction on the quality factor of micro-beam resonators. *Microsystem Technologies*, 23(8), 3489–3504.
35. Nguyen, C. C., & Li, W. L. (2017). Influences of temperature on the quality factors of micro-beam resonators in gas rarefaction. *Sensors and Actuators A: Physical*, 261, 151–165.
36. Nguyen, C. C., Ngo, V. K. T., Le, H. Q., & Li, W. L. (2018). Influences of relative humidity on the quality factors of MEMS cantilever resonators in gas rarefaction. *Microsystem Technologies*, 25, 2767–2782.
37. Hosseinian, E., Theillet, P. O., & Pierron, O. N. (2013). Temperature and humidity effects on the quality factor of a silicon lateral rotary micro-resonator in atmospheric air. *Sensors and Actuators A: Physical*, 189, 380–389.
38. Nieva, P. M., McGruer, N. E., & Adams, G. G. (2006). Design and characterization of a micromachined fabry-perot vibration sensor for high-temperature applications. *Journal of Micromechanics and Microengineering*, 16(12), 2618–2631.
39. Hosseinzadegan, H., Pierron, O. N., & Hosseinian, E. (2014). Accurate modeling of air shear damping of a silicon lateral rotary micro-resonator for MEMS environmental monitoring applications. *Sensors and Actuators A: Physical*, 216, 342–348.
40. Jan, M. T., Ahmad, F., Hamid, N. H. B., Khir, M. H. B. M., Shoaib, M., & Ashraf, K. (2016). Experimental investigation of moisture and temperature effects on resonance frequency and quality factor of CMOS-MEMS paddle resonator. *Microelectronics Reliability*, 63, 82–89.
41. Hwang, C. C., Fung, R. F., Yang, R. F., Weng, C. I., & Li, W. L. (1996). A new modified Reynolds equation for ultrathin film gas lubrication. *IEEE Transactions on Magnetics*, 32(2), 344–347.
42. Li, W. L. (1999). Analytical modelling of ultra-thin gas squeeze film. *Nanotechnology*, 10(4), 440–446.
43. Li, W. L. (2002). A database for couette flow rate considering the effects of non-symmetric molecular interactions. *Journal of Tribology*, 124(4), 869–873.
44. Li, W. L. (2003). A database for interpolation of Poiseuille flow rate for arbitrary Knudsen number lubrication problems. *Journal of the Chinese Institute of Engineers*, 26(4), 455–466.
45. Li, W. L. (2004). Modeling of head/disk interface—an average flow model. *Tribology Letters*, 17, 669–676.
46. Li, W. L. (2008). Squeeze film effects on dynamic performance of MEMS μ -mirrors—consideration of gas rarefaction and surface roughness. *Microsystem Technologies*, 14(3), 315–324.
47. Hasan, M. H. (2018). Influence Of Environmental Conditions On The Response Of MEMS Resonators, *Dissertation*, University of Nebraska.

48. Morvay, Z. K., & Gvozdenac, D. D. (2008). Applied Industrial Energy and Environmental Management. in: *Fundamentals for analysis and calculation of energy and environmental performance*, (pp. 1–5), Wiley, Ltd.
49. Kreith, F., & Goswami, D. Y. (2005). The CRC HANDBOOK of Mechanical engineering. In: *CRC Press LLC*, (pp. 1385).
50. Tan, Z. (2014). Air pollution and greenhouse gases. *Springer Science + Business Media*, (pp. 33–34), Singapore.
51. ASHRAE. (2001). The 2001 ASHRAE Fundamentals Handbook. (pp. 6.2).
52. Sarairoh M. (2012). Heat transfer and condensation of water vapour from humid air in compact heat exchangers. *Doctor of Philosophy*, Victoria University, (pp. 67), Footscray.
53. Leissa, A. W. (1969). Vibration of Plates, In: *NASA*, (pp. 1–6), Washington DC.
54. Nayfeh, A. H., & Younis, M. I. (2004). A new approach to the modeling and simulation of flexible microstructures under the effect of squeeze film damping. *Journal of Micromechanics and Microengineering*, 14, 170–181.
55. COMSOL Multiphysics 5.5. (2021). Thermoelastic damping in a MEMS resonator, <https://www.comsol.com/model/thermoelastic-damping-in-a-mems-resonator-1439>. License Date to February 1, 2021.
56. Matthew, A. H., William, D. N., & Thomas, W. K. (2010). What is the young's modulus of silicon? *Journal of Microelectromechanical Systems*, 19(2), 229–238.

Publisher's Note Springer Nature remains neutral with regard to jurisdictional claims in published maps and institutional affiliations.

Affiliations

Minh Truong Phan¹ · Xuan Thang Trinh² · Quoc Cuong Le³ · Vo Ke Thanh Ngo² · Chi Cuong Nguyen^{1,2} 

¹ Institute for Computational Science and Technology, Room 311(A&B), SBI building, Quang Trung Software City, Tan Chanh Hiep ward, District 12, Ho Chi Minh City, Vietnam

² The Research Laboratories of Saigon High-Tech-Park, Lot I3, N2 Street, Saigon Hi-Tech-Park, District 9, Ho Chi Minh City, Vietnam

³ Department of Information and Communications, 59 Ly Tu Trong street, Ben Nghe ward, District 1, Ho Chi Minh City, Vietnam

Terms and Conditions

Springer Nature journal content, brought to you courtesy of Springer Nature Customer Service Center GmbH (“Springer Nature”).

Springer Nature supports a reasonable amount of sharing of research papers by authors, subscribers and authorised users (“Users”), for small-scale personal, non-commercial use provided that all copyright, trade and service marks and other proprietary notices are maintained. By accessing, sharing, receiving or otherwise using the Springer Nature journal content you agree to these terms of use (“Terms”). For these purposes, Springer Nature considers academic use (by researchers and students) to be non-commercial.

These Terms are supplementary and will apply in addition to any applicable website terms and conditions, a relevant site licence or a personal subscription. These Terms will prevail over any conflict or ambiguity with regards to the relevant terms, a site licence or a personal subscription (to the extent of the conflict or ambiguity only). For Creative Commons-licensed articles, the terms of the Creative Commons license used will apply.

We collect and use personal data to provide access to the Springer Nature journal content. We may also use these personal data internally within ResearchGate and Springer Nature and as agreed share it, in an anonymised way, for purposes of tracking, analysis and reporting. We will not otherwise disclose your personal data outside the ResearchGate or the Springer Nature group of companies unless we have your permission as detailed in the Privacy Policy.

While Users may use the Springer Nature journal content for small scale, personal non-commercial use, it is important to note that Users may not:

1. use such content for the purpose of providing other users with access on a regular or large scale basis or as a means to circumvent access control;
2. use such content where to do so would be considered a criminal or statutory offence in any jurisdiction, or gives rise to civil liability, or is otherwise unlawful;
3. falsely or misleadingly imply or suggest endorsement, approval, sponsorship, or association unless explicitly agreed to by Springer Nature in writing;
4. use bots or other automated methods to access the content or redirect messages
5. override any security feature or exclusionary protocol; or
6. share the content in order to create substitute for Springer Nature products or services or a systematic database of Springer Nature journal content.

In line with the restriction against commercial use, Springer Nature does not permit the creation of a product or service that creates revenue, royalties, rent or income from our content or its inclusion as part of a paid for service or for other commercial gain. Springer Nature journal content cannot be used for inter-library loans and librarians may not upload Springer Nature journal content on a large scale into their, or any other, institutional repository.

These terms of use are reviewed regularly and may be amended at any time. Springer Nature is not obligated to publish any information or content on this website and may remove it or features or functionality at our sole discretion, at any time with or without notice. Springer Nature may revoke this licence to you at any time and remove access to any copies of the Springer Nature journal content which have been saved.

To the fullest extent permitted by law, Springer Nature makes no warranties, representations or guarantees to Users, either express or implied with respect to the Springer nature journal content and all parties disclaim and waive any implied warranties or warranties imposed by law, including merchantability or fitness for any particular purpose.

Please note that these rights do not automatically extend to content, data or other material published by Springer Nature that may be licensed from third parties.

If you would like to use or distribute our Springer Nature journal content to a wider audience or on a regular basis or in any other manner not expressly permitted by these Terms, please contact Springer Nature at

onlineservice@springernature.com